Chemical Engineering Journal 232 (2013) 81–88

Contents lists available at ScienceDirect

Chemical Engineering Journal

journal homepage: www.elsevier.com/locate/cej

Experimental study on oxidation of elemental mercury by UV/Fenton system

Fuman Zhan, Caiting Li *, Guangming Zeng, Shasha Tao, Yujun Xiao, Xing Zhang, Lingkui Zhao, Jie Zhang, Jinfeng Ma

College of Environmental Science and Engineering, Hunan University, Changsha 410082, PR China
Key Laboratory of Environmental Biology and Pollution Control (Hunan University), Ministry of Education, Changsha 410082, PR China

HIGHLIGHTS

- UV/Fenton system was developed for effective Hg^0 oxidation from simulated flue gas.
- The reaction mechanism of Hg^0 with $^{\cdot}OH$ and $HO_2^{\cdot}$ was presented.
- The mechanism of Hg^0 secondary volatile by SO_2 was studied.
- The roles of flue gas components in Hg^0 oxidation by UV/Fenton system were explored.

ARTICLE INFO

Article history:
Received 31 March 2013
Received in revised form 3 July 2013
Accepted 20 July 2013
Available online 27 July 2013

Keywords:
Mercury
Fenton's reagent
Free radicals
WFGD

ABSTRACT

In order to implement Hg^0 control strategy in a wet scrubber, oxidation of elemental mercury (Hg^0) in the simulated coal-fired flue gas by UV/Fenton system was investigated. Effects of different operation parameters have been studied, including initial solution pH, H_2O_2, TiO_2 and Fe^{2+} concentration, solution temperature, gas flow rate and flue gas components (O_2, SO_2 and NO). The main ion products in the solution have been analyzed. The experimental results suggested that oxidation of Hg^0 was inhibited with the increase of initial solution pH and gas flow rate. Additionally, with the increase of the H_2O_2, TiO_2, Fe^{2+} concentration and solution temperature, the Hg^0 oxidation efficiency was enhanced to the maximum at first and then decreased. Hg^0 oxidation can be significantly inhibited by SO_2 and NO when the flue gas was absence of O_2, but the oxidation capacity was recovered with 9% O_2 exist in the flue gas. SO_2 showed an inhibition effect on Hg^0 oxidation, while the inhibition was weakened at higher SO_2 concentration. Different NO concentration had an insignificant effect on Hg^0 oxidation process under the experimental conditions. In the case of presence and absence of flue gas components (9% O_2, 800 ppm SO_2, 600 ppm NO) and under the optimal conditions ($pH = 1$, $[H_2O_2] = 0.05$ mol/L; $[TiO_2] = 0.6$ g/L; $[Fe^{2+}]/[H_2O_2] = 1/2$; $T = 40$ °C), the average oxidation efficiency of Hg^0 can reach to 94.4% and 98.5%, respectively.

1. Introduction

Mercury, a trace element exists in the coal and other potential fossil fuels, can be released into the atmosphere during the combustion of these materials [1]. Due to the characteristics of toxicity, persistent bioaccumulation, high volatility and nearly insolubility in water [1–3], mercury has been regarded as a global pollutant and received a significant attention around the world. Compared with the mercury emitted from nature sources, anthropogenic discharged has become the main source of mercury emission [4]. While coal-fired power plants have been accounted for about one third of the anthropogenic emission sources due to the large quantity of coal used for electricity generation [1,4]. As a result, the control of mercury emitted from coal-fired power plants has been seriously concerned. On December 21, 2011 the US Environment Protection Agency (EPA) has announced the Mercury and Air Toxics Standards (MATS) to control the mercury, acid gases and other toxic pollution from coal-fired power plants and the final rule was effective on April 16, 2012 [5]. Therefore, it has become an extremely urgent task at present to improve the removal efficiency of mercury from coal-fired flue gas.

Mercury in the coal-derived flue gas is present in three forms, i.e. elemental mercury (Hg^0), oxidized mercury (Hg^{2+}) and particle-bound mercury (Hg^p) [6–8]. Hg^p can be captured along with fly ash particles by electrostatic precipitators (ESPs) or fabric filters (FFs) [9]. Water-soluble Hg^{2+} can be readily removed with SO_2 from the gas steam by wet flue gas desulfurization (WFGD) equipments and the Hg^{2+} removal efficiency can reach to 90% [2,8,10].

---

* Corresponding author at: College of Environmental Science and Engineering, Hunan University, Changsha 410082, PR China. Tel./fax: +86 731 88649216.
E-mail addresses: ctli@hnu.edu.cn, ctli3@yahoo.com (C. Li).

1385-8947/$ - see front matter © 2013 Elsevier B.V. All rights reserved.
http://dx.doi.org/10.1016/j.cej.2013.07.082

Conversely, it is difficult to directly remove Hg^0 from flue gas by these conventional air pollution control devices because of its high volatility, stability and nearly insolubility in water [3,8]. Thus Hg^0 has become the dominant mercury species emitted into the atmosphere [11]. As can be seen from the above presentation, the removal of mercury will be enhanced when Hg^0 is converted to its oxidized form.

To date, lots of technologies have been developed to remove Hg^0 from the flue gas. Heterogeneous catalytic oxidation of mercury using carbon-based catalysts, SCR catalysts and metals or metal oxides have been largely reported in the literature in recent years [6,9,12]. Photochemical oxidation utilizing ultraviolet and visible light, which show a promising performance in heterogeneous oxidation of Hg^0, has also been investigated by researchers [13,14]. Oxidation of Hg^0 by Cl_2, Br_2, chlorine radicals, O_3, $K_2S_2O_8$, $NaClO_2$ and $KMnO_4$ has been explored and shown a relatively high efficiency of mercury oxidation [10,15–20].

The limestone-based wet scrubbing is still to be the most effective and widely used process for SO_2 control in the coal-fired power plants at home and abroad [21]. The enhancement in oxidation of Hg^0 to more soluble Hg^{2+}, which can be simultaneously captured with SO_2 by the WFGD, has drawn increasing attention in last years [6,22]. Hydroxyl radicals ($\cdot OH$), which is a kind of strong oxidant produced by the advanced oxidation processes (AOPs), can react non-selectively with many environmental contaminations and simultaneously remove multiple pollutants from flue gas [23–25]. As one of the promising AOPs, Fenton reaction has become a powerful and efficient technique to co-effectively eliminate environmental pollutants [26]. Moreover, the non-selective oxidation of Fenton's reagent has showed unique advantages and promising applied prospects in the area of disposal of wastewater and waste gas [23–25,27,28]. It has been reported that the degradation of pollutants can be obviously improved when ultraviolet light (UV) and TiO_2 is introduced into the Fenton system [29,30]. Until now, using Fenton's reagent for mercury oxidation has rarely been reported in the literature. In this paper, removal of elemental mercury from the simulated flue gas was studied in a lab-scale bubble reactor and the effects of different operation parameters on Hg^0 oxidation efficiency have been investigated, including initial solution pH value, H_2O_2, TiO_2 and Fe^{2+} concentration, solution temperature, flue gas flow rate and flue gas components (O_2, SO_2 and NO). The results may be able to provide some theoretical reference for the development and application of removal of Hg^0 and SO_2 as well as NO by wet scrubber with UV/Fenton system.

2. Experimental

2.1. Reagents

All the reagents used in this work were analytical pure grade (AR), including: ferrous chloride (99.5%, Guangdong, China), hydrogen peroxide (30.0%, w/w, Changsha, China), Titanium dioxide (99.0%, Tianjin, China), sodium hydroxide (96.0%, Tianjin, China) and hydrogen chloride (36–38%, w/w, Zhuzhou, China). Ultrapure water was applied to prepare the required solutions.

2.2. Experimental apparatus

Experimental system is shown in Fig. 1. The experimental apparatus consisted of a flue gas simulation system, a mercury generation system, an absorption bubble reactor, an online gas analysis system and a waste gas treatment system.

The composition of basic flue gas included, N_2 (99.999%), O_2 (99.999%), NO (20.0%NO + 80.0%N_2) and SO_2 (20.4%SO_2 + 79.6%N_2). Before the reactor, a buffer tank was used to mix the different gas and the total gas flow rate was controlled by the mass flow controllers (MFC, Beijing Seven-Star Electronics Co., Ltd., China). The elemental mercury was generated by a mercury permeation tube (VICI Metronics Co., USA) which was placed in a U-shaped glass and heated in a thermostatic water bath.

The body of the photochemical reactor was a bubble column reactor (height, 200 mm; inside diameter, 80 mm) and two UV lamps (254 nm, 20 W) were placed at both sides of the reactor. A thermostatic magnetic stirrer was used for the purpose of homogeneous mixing and temperature regulating of the solution.

In order to protect the mercury online analyzer, an ice bath condenser following by the reactor was used to remove the moisture content in the simulated flue gas. The inlet and outlet concentration of Hg^0 was monitored by a RA-915M Mercury Analyzer (Lumex Co., Ltd., Russia) with a detection limit of 2 ng/m^3. The gas from the mercury analyzer was introduced into an activated carbon trap before being expelled into the atmosphere.

2.3. Experimental procedure

Firstly, the basic gas was used to make up the simulated flue gas. The N_2 flow was divided into two branches: one branch, as the balance gas, converged with the O_2, NO and SO_2 in the buffer tank, while the other (200 mL/min) passed through the mercury permeation tube as a carrier gas to introduce a steady Hg^0 vapor into the buffer tank. In this study, the temperature of the mercury permeation tube was selected as 80 °C and the corresponding Hg^0 concentration in the simulated flue gas was about 105 μg/m^3.

Then, Fenton solution was freshly prepared with H_2O_2 solution, $FeCl_2 \cdot 4H_2O$, TiO_2 and ultrapure water according to the required concentration of H_2O_2, Fe^{2+} and TiO_2. The volume of solution used for each experiment was 500 mL. Before the experiments the initial solution pH value was adjusted through HCl (0.5 mol/L) and NaOH (0.5 mol/L) and measured by an acidometer (Shanghai leici instrument Co., China).

Furthermore, the experiments were conducted after the inlet concentration of Hg^0 was steady. The gas mixture continuously flowed through the UV/Fenton system and the reaction time of each experiment was maintained for 2 h in this study. During the experiments, the concentration of Hg^0 in the gas bypass (A) and the gas primary road (B) was measured before and after the absorption processes to calculate the oxidation efficiency of Hg^0.

In this study, a sequence of experiments was carried out to evaluate the effect of different operational parameters on Hg^0 oxidation efficiency in a bubble reactor. The range of experimental conditions for the experiments is shown in Table 1. The oxidation efficiency was calculated by the following equation:

$$\eta(\%) = \frac{C_{in} - C_{out}}{C_{in}} \times 100\% \qquad (1)$$

where η is the oxidation efficiency of Hg^0, C_{in} and C_{out} represent the average Hg^0 concentration at the inlet and outlet of the reactor, respectively.

The experimental error is inevitable. Hence, η is the average of three replicates and the error bars in the figures represent the standard deviation from the mean of the series of experiments at each condition.

3. Results and discussion

3.1. Reaction mechanisms

The mechanisms between Hg^0 and Fenton's reagent are considered as the following reactions:

(1) Fenton reaction [22,29]:

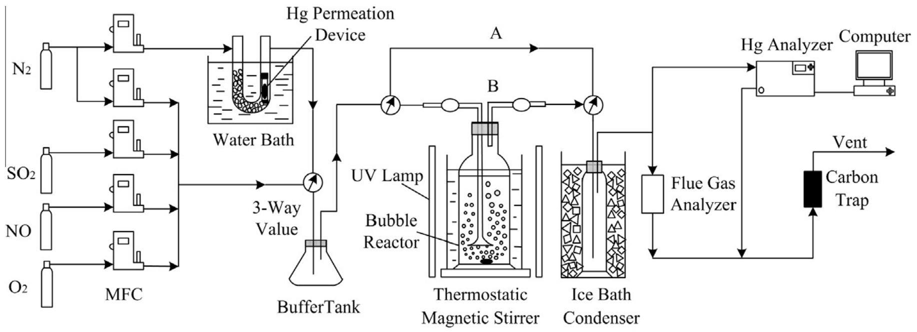

Fig. 1. Schematic diagram of the experimental system.

Table 1
The experimental parameters and conditions.

Operating parameters	Range of operation	Experiment conditions
Initial solution pH value	1–5	$[H_2O_2]$ = 0.1 mol/L; $[TiO_2]$ = 0.6 g/L; $[Fe^{2+}]$ = 0.05 mol/L; T = 40 °C; Q (Gas flow rate) = 500 mL/min; C_{in} (Inlet Hg^0 concentration) = 105 μg/m^3 and balance N_2
H_2O_2 concentration	0–0.4 mol/L	The above optimized parameters
TiO_2 concentration	0–1.0 g/L	The above optimized parameters
$[Fe^{2+}]/[H_2O_2]$	0–2	The above optimized parameters
Reaction temperature	30–70 °C	The above optimized parameters
The gas flow rate	200–1200 mL/min	The above optimized parameters
O_2 concentration	0–12%	The above optimized parameters + 800ppmSO_2 + 600ppmNO
SO_2 concentration	0–1000 ppm	The above optimized parameters + 9%O_2 + 600ppmNO
NO concentration	0–800 ppm	The above optimized parameters + 9%O_2 + 800ppmSO_2

$$Fe^{2+} + H_2O_2 \rightarrow Fe^{3+} + OH^- + {\cdot}OH \quad (2)$$

$$Fe^{3+} + H_2O_2 \rightarrow Fe^{2+} + H^+ + HO_2^{\cdot} \quad (3)$$

When the UV irradiation was introduced, the generation rate of ·OH and $HO_2^{\cdot}$ free radicals would be enhanced by the following reactions [31–33]:

$$H_2O_2 \xrightarrow{hv} 2{\cdot}OH \quad (4)$$

$$Fe^{3+} + H_2O \xrightarrow{hv} {\cdot}OH + Fe^{2+} + H^+ \quad (5)$$

$$TiO_2 \xrightarrow{hv(<380nm)} h^+ + e^- \quad (6)$$

$$h^+ + H_2O \rightarrow H^+ + {\cdot}OH \quad (7)$$

$$e^- + H_2O_2 \rightarrow OH^- + {\cdot}OH \quad (8)$$

(2) It has been generally accepted that ·OH and $HO_2^{\cdot}$ are the main intermediate in Fenton reaction, and the main reactions between Hg^0 and these free radicals could be written as [10,22]:

$$Hg^0 + 2{\cdot}OH + 2H^+ \rightarrow Hg^{2+} + 2H_2O \quad (9)$$

$$2Hg^0 + 2HO_2{\cdot} + 2H^+ \rightarrow Hg_2^{2+} + 2H_2O_2 \quad (10)$$

$$Hg_2^{2+} + 2HO_2{\cdot} + 2H^+ \rightarrow 2Hg^{2+} + H_2O_2 \quad (11)$$

3.2. Effect of initial pH value

The experiments were carried out at a pH value within the range of 1–5 and effect of initial solution pH value on Hg^0 oxidation efficiency is shown in Table 2. The Hg^0 oxidation efficiency decreased with the increase of initial solution pH value and the average oxidation efficiencies were about 96.57%, 88.05% and 79.08% for the initial solution pH values of 1, 2 and 3, respectively. However, when the pH value further increased to 5, the average oxidation efficiency decreased rapidly to about 45.03%. It was obvious that the initial solution pH value had a significant impact on Hg^0 oxidation and a suitable solution pH window was found between 1 and 3, which was in agreement with the findings of Dennis Lu [22].

At a pH value lower than 3, the oxidation of Hg^0 can be promoted due to the consumption of H^+ by the redox reactions (Eqs. (2), (9)–(11)). Therefore the decrease of initial solution pH value was beneficial for Hg^0 oxidation. However, the iron in the solution will be precipitated as hydroxide when the solution pH value is higher than 3.5 [26], which would reduce the transmission of ultraviolet radiation, resulting in not taking full advantages of ultraviolet radiation. Additionally, the oxidation potential of ·OH is decreased with the increase of the solution pH value (E^0 = 2.8 V and E^{14} = 1.95 V) [34]. As a result, the mercury oxidation efficiency was decreased with the increase of solution pH value. So the Hg^0 oxidation can be promoted considering that the pH value of WFGD system decreases with the absorption SO_2, which was consistent with the results of Fig. 3.

3.3. Effect of H_2O_2 concentration

The effect of H_2O_2 concentration on Hg^0 oxidation efficiency was preliminarily studied and the results are shown in Table 2. It can be seen that initial concentration of H_2O_2 played an essential role in the Fenton process. There was neglected efficiency on Hg^0 oxidation in the absence of H_2O_2. When the H_2O_2 concentration rose to 0.02 mol/L and 0.05 mol/L, Hg^0 oxidation efficiency jumped to 75.88% and 97.94%, respectively. But as the H_2O_2 concentration further increased from 0.1 to 0.4 mol/L, Hg^0 oxidation efficiency saw a slightly fall from 96.89% to 91.13%.

Increasing of H_2O_2 concentration within a certain range can facilitate the yield of ·OH and $HO_2^{\cdot}$ radicals (Eqs. (2)–(4)), which

Table 2
The effects of experimental parameters on Hg^0 oxidation.

The range of pH value	1	2	3	4	5		
Average oxidation efficiencies of Hg^0 (%)	96.57	88.05	79.08	66.08	45.03		
The range of H_2O_2 concentration (mol/L)	0	0.02	0.05	0.10	0.20	0.30	0.40
Average oxidation efficiencies of Hg^0 (%)	6.62	75.88	97.94	96.89	93.22	92.57	91.13
The range of TiO_2 concentration (g/L)	0	0.2	0.4	0.6	0.8	1.0	
Average oxidation efficiencies of Hg^0 (%)	92.94	93.46	95.85	97.51	94.47	88.65	
The range of $[Fe^{2+}]/[H_2O_2]$ ratio	0	1/12	1/8	1/4	1/2	1	2
Average oxidation efficiencies of Hg^0 (%)	76.59	89.86	92.58	96.58	98.43	97.64	32.68
The range of solution temperature (°C)	30	40	50	60	70		
Average oxidation efficiencies of Hg^0 (%)	96.82	98.36	92.11	84.96	70.93		
The range of gas flow rate (mL/min)	200	400	600	800	1000	1200	
Average oxidation efficiencies of Hg^0 (%)	99.14	98.87	97.41	94.21	91.32	89.46	

was finally advantageous to the oxidation of Hg^0. However, when H_2O_2 concentration exceeded the optimal value, the quantity of $^{\cdot}OH$ and $HO_2^{\cdot}$ free radicals greatly increased in the solution. Then several side reactions (Eqs. (12)–(17)) would take place and accelerate, leading to the great self-loss of $^{\cdot}OH$ and $HO_2^{\cdot}$ free radicals [24,25,35,36]. Consequently there was no positive effect on the Hg^0 oxidation with further increase of the H_2O_2 concentration. As a result, the optimal H_2O_2 concentration in this study was selected as 0.05 mol/L.

$$^{\cdot}OH + ^{\cdot}OH \rightarrow H_2O_2 \tag{12}$$

$$^{\cdot}OH + HO_2^{\cdot} \rightarrow H_2O + O_2 \tag{13}$$

$$^{\cdot}OH + O_2^{-} \rightarrow OH^{-} + O_2 \tag{14}$$

$$HO_2^{\cdot} + HO_2^{\cdot} \rightarrow H_2O_2 + O_2 \tag{15}$$

$$Fe^{2+} + ^{\cdot}OH \rightarrow Fe^{3+} + OH^{-} \tag{16}$$

$$Fe^{3+} + HO_2^{\cdot} \rightarrow Fe^{2+} + H^{+} + O_2 \tag{17}$$

3.4. Effect of TiO_2 concentration

A series of experiments were performed to investigate the effect of TiO_2 concentration on Hg^0 oxidation efficiency. The experimental results are shown in Table 2. It was observed from Table 2 that with the increase of TiO_2 concentration from 0 to 0.6 g/L, Hg^0 oxidation efficiency increased from 92.94% to 97.51%. However, when the TiO_2 concentration further increased from 0.8 to 1.0 g/L, Hg^0 oxidation efficiency had a decrease from 94.47% to 88.65%.

This observation can be explained by the availability of active sites on the TiO_2 surface and the penetration of ultraviolet light into the suspension. The availability of active sites increases with the rise of TiO_2 dosage [33], which excited to produced high-energy states of electron and hole pairs under the illumination of UV light (Eq. (6)). The generated hole reacts with electron donors to produce strong oxidizing $^{\cdot}OH$ (Eq. (7)) then promoted the oxidation of elemental mercury. The H_2O_2 in the solution accept a photo-generated electron from the conduction band, which result in promoting the charge separation and the production of $^{\cdot}OH$ (Eq. (8)) in the process of photo-catalytic oxidation. Therefore, the increasing of TiO_2 dosage can finally enhance the oxidation of Hg^0. However, with the increase of TiO_2 concentration, the UV-light transmission would be reduced and the light scattering would be enhanced by the suspended particles [32]. Furthermore, the potential agglomeration of the TiO_2 particles in the solution would result in a loss of surface area available for light-harvesting, which may lead to the decrease of oxidation efficiency at high TiO_2 concentration [37]. Thus, any further increase of TiO_2 concentration after the optimal dosage may have an inhibition effect on the mercury oxidation. The optimum amount of TiO_2 was added into the solution in order to avoid unnecessary excess waste and also to ensure total absorption of light photons for Hg^0 oxidation. In this study, the optimal TiO_2 concentration is selected as 0.6 g/L.

3.5. Effect of Fe^{2+} concentration

The amount of ferrous ion is one of the main parameters to influence the Fenton process. Different initial concentration of Fe^{2+} at a fixed H_2O_2 concentration of 0.05 mol/L has been experimented in order to obtain the optimal initial concentration ratio of $[Fe^{2+}]/[H_2O_2]$ and the tests were conducted by changing the $[Fe^{2+}]/[H_2O_2]$ ratio within the range of 0–2. The experimental results are shown in Table 2 and it indicated that with the increase of initial $[Fe^{2+}]/[H_2O_2]$ ratio from 0 to 1/2 the efficiency of Hg^0 oxidation had a sharp increase from 76.59% to 98.43%. Further increased of the $[Fe^{2+}]/[H_2O_2]$ ratio from 1 to 2, the Hg^0 oxidation efficiency had a significant declination from 97.64% to 32.68%.

It has been known that Fe^{2+} had a catalytic decomposition effect on H_2O_2 to generate $^{\cdot}OH$ and $HO_2^{\cdot}$ free radicals (Eqs. (2) and (3)). Increasing Fe^{2+} concentration promoted the yield of $^{\cdot}OH$ free radicals in the UV/Fenton system (Eq. (2)), thereby improving the oxidation of Hg^0. However, adding excessive Fe^{2+} can also result in a great self-consumption of $^{\cdot}OH$ and $HO_2^{\cdot}$ free radicals which was caused by side reactions (Eqs. (16) and (17)) [38], therefore inhibiting the oxidation of Hg^0. Thus, the optimal ratio of $[Fe^{2+}]/[H_2O_2]$ was selected as 1/2 for the oxidation of Hg^0 by the UV/Fenton treatments in this study.

3.6. Effect of solution temperature

The effect of solution temperature on the oxidation of Hg^0 has been studied at temperatures range from 30 to 70 °C. The results obtained are shown in Table 2. It clearly indicated that the Hg^0 oxidation efficiency firstly went up with the increase of the solution temperature from 30 °C to 40 °C. But it experienced a sharp decline with the further increase of the solution temperature to 70 °C.

The generation of $^{\cdot}OH$ and $HO_2^{\cdot}$ can be promoted by the increase of reaction temperature [23], which would benefit to the oxidation of Hg^0. However, due to the poor stability of H_2O_2 at high temperature, the decomposition of H_2O_2 (Eq. (18)) would be accelerated by the increase of reaction temperature, which was not favorable to the formation of $^{\cdot}OH$ and resulted in lower Hg^0 oxidation efficiency. Similar results were reported by Samet et al. [26].

$$2H_2O_2 \rightarrow 2H_2O + O_2 \tag{18}$$

3.7. Effect of gas flow rate

The effect of the gas flow rate on Hg^0 oxidation efficiency has been investigated in the range of 200–1200 mL/min and the results are shown in Table 2. It can be seen that the gas flow rate had a slight impact on Hg^0 oxidation efficiency. With an increase of the gas flow rate from 200 to 1200 mL/min, the oxidation efficiency showed a decline from 99.14% to 89.46%.

At lower gas flow rate, the gas–liquid mass-transfer rate can be promoted by increasing the gas flow rate, thereby facilitating the absorption of Hg^0. However, the increase of the gas flow rate would reduce the residence time (reaction time) of Hg^0 in the solution. In addition, the amount of Hg^0 entering into the reactor per unit time greatly increased by increasing the gas flow rate, which can decrease the relative molar ratio of $^{\cdot}OH$ and $HO_2^{\cdot}$ to Hg^0, thereby leading to the reduction of Hg^0 oxidation efficiency. From the analysis mentioned above, the latter factor might play a leading role in the reaction process. As a result, the Hg^0 oxidation efficiency decreased with the increase of the gas flow rate.

3.8. Effects of flue gas components

As the main components of the coal-fired flue gas, O_2, SO_2 and NO may have a certain influence on Hg^0 oxidation process. To explore the roles of flue gas components in Hg^0 oxidation, experiments were conducted under the optimal parameters (pH = 1, $[H_2O_2] = 0.05$ mol/L; $[TiO_2] = 0.6$ g/L; $[Fe^{2+}]/[H_2O_2] = 1/2$; $T = 40$ °C), by mixing Hg^0 with O_2, SO_2, NO and balance N_2. The concentrations of O_2, SO_2 and NO in the simulated flue gas were referred to the range of which in the real flue gas.

3.8.1. Effect of O_2

The effect of O_2 on Hg^0 oxidation by UV/Fenton system was examined and the results are given in Fig. 2. It could be seen that when the O_2 concentration rose from 0% to 9%, the averaged Hg^0 oxidation efficiency increased sharply from 74.50% to 95.32%. It indicated that the increase of O_2 concentration to a certain value was favorable to the Hg^0 oxidation process. However, when the O_2 concentration continuously increased to 12%, the averaged Hg^0 oxidation efficiency had a sharp decrease to 22.20%. In addition, it also suggested that, in the absence of O_2, the existence of 800 ppm SO_2 and 400 ppm NO in the flue gas has a great suppressed on the Hg^0 oxidation efficiency when compared with the results of solution temperature in Table 2.

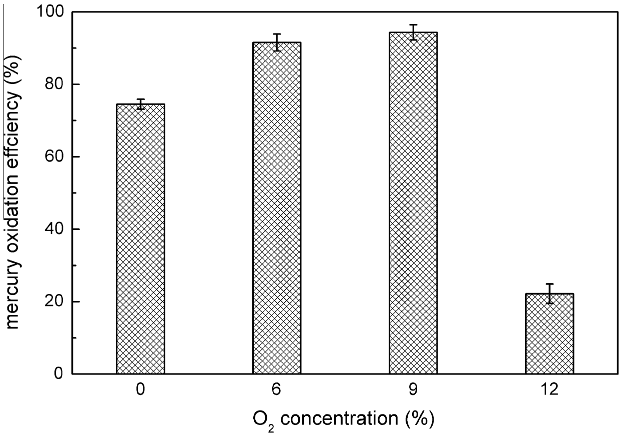

Fig. 2. Effect of the O_2 concentration on Hg^0 oxidation efficiency. Conditions: pH = 1; $[H_2O_2] = 0.05$ mol/L; $[Fe^{2+}]/[H_2O_2] = 1/2$; $[TiO_2] = 0.6$ g/L; $T = 40$ °C; $Q = 500$ mL/min; 800 ppm SO_2; 600 ppm NO; $C_{in} = 105$ μg/m^3 and balance N_2.

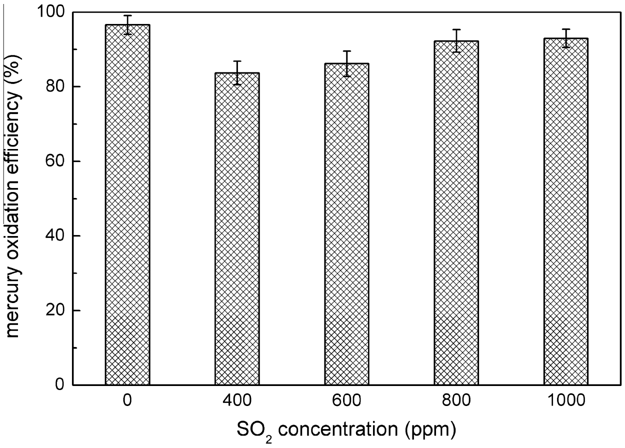

Fig. 3. Effect of the SO_2 concentration on Hg^0 oxidation efficiency. Conditions: pH = 1; $[H_2O_2] = 0.05$ mol/L; $[Fe^{2+}]/[H_2O_2] = 1/2$; $[TiO_2] = 0.6$ g/L; $T = 40$ °C; $Q = 500$ mL/min; 9% O_2; 600 ppm NO; $C_{in} = 105$ μg/m^3 and balance N_2.

It indicated that the introduction of O_2 to the UV/Fenton system was conductive to the mercury oxidation, which was due to the enhancement of $^{\cdot}OH$ and $HO_2^{\cdot}$ generation by the synergies of O_3 and H_2O_2 (Eqs. (19)–(22)) [39].

$$O_2 \xrightarrow{h\upsilon} O_3 \xrightarrow{h\upsilon} O + O_2 \tag{19}$$

$$O + H_2O \rightarrow H_2O_2 \xrightarrow{h\upsilon} 2{}^{\cdot}OH \tag{20}$$

$$O_3 + H_2O \xrightarrow{h\upsilon} H_2O_2 + O_2 \tag{21}$$

$$O_3 + H_2O_2 \rightarrow HO_2{}^{\cdot} + {}^{\cdot}OH + O_2 \tag{22}$$

However, the oxidation efficiency was suppressed when the concentration of O_2 exceeded 9%. This was because of the fact that the generation of O_3 growth with the increase of O_2 concentration, resulting in the excess of $^{\cdot}OH$ and $HO_2^{\cdot}$ generation, which would cause side reactions (Eqs. (12)–(13) and (15)) to induce the $^{\cdot}OH$ and $HO_2^{\cdot}$ radical scavenging effect. As a result, the oxidation process was inhibited by the further increase of O_2 concentration. The optimal O_2 concentration was chosen as 9% in this study.

3.8.2. Effect of SO_2

The influence of SO_2 concentration on Hg^0 oxidation was investigated by a series of experiments and the results are shown in Fig. 3. Under the experimental conditions, the average oxidation efficiencies of Hg^0 were about 95.59%, 83.71%, 86.19%, 92.19% and 92.87% with the SO_2 concentration of 0, 400, 600, 800 and 1000 ppm, respectively. The average Hg^0 oxidation efficiency was inhibited by adding SO_2 into the system. However, the inhibited effect was weakened with the increase of SO_2 concentration.

Water-soluble SO_2 was very easy to dissolve into the Fenton's reagent and some products like SO_3^{2-} and HSO_3^- were generated by the reaction between SO_2 and H_2O. These reaction products and SO_2 can further react with H_2O_2 and $\cdot OH{}^{\cdot}OH$, as shown in the following reactions (Eqs. (23)–(27)) [25,40,41]. These reactions consumed a great amount of H_2O_2 and $^{\cdot}OH$, resulting in the underutilization of H_2O_2 and $^{\cdot}OH$.

$$SO_2 + H_2O_2 \rightarrow 2H^+ + SO_4^{2-} \tag{23}$$

$$SO_2 + 2{}^{\cdot}OH \rightarrow 2H^+ + SO_4^{2-} \tag{24}$$

$$HSO_3^- + {}^{\cdot}OH \rightarrow {}^{\cdot}SO_3^- + H_2O \tag{25}$$

$$HSO_3^- + H_2O_2 \rightarrow HSO_4^- + H_2O \quad (26)$$

$$SO_3^{2-} + H_2O_2 \rightarrow SO_4^{2-} + H_2O \quad (27)$$

Additionally, large number of HSO_3^- and SO_3^{2-} existing in the system can react with Hg^{2+} in the solution, leading to the secondary volatile of Hg^0 (Eqs. (28)–(30)) [42].

$$Hg^{2+} + HSO_3^- + H_2O \rightarrow Hg^0 \uparrow + SO_4^{2-} + 3H^+ \quad (28)$$

$$Hg^{2+} + SO_3^{2-} \leftrightarrow HgSO_3 \quad (29)$$

$$HgSO_3 + H_2O \rightarrow Hg^0 \uparrow + SO_4^{2-} + 2H^+ \quad (30)$$

$$HgSO_3 + SO_3^{2-} \leftrightarrow Hg(SO_3)_2^{2-} \quad (31)$$

However, with excess sulfite in the solution, the major mercuric species was thought to be the more stabled $Hg(SO_3)_2^{2-}$ (Eq. (31)) and the formation of that was promoted at temperatures below 45 °C, resulting in inhibiting the reduction of $HgSO_3$ to Hg^0 [43]. In addition, when a large number of HSO_3^- and SO_3^{2-} in the solution were oxidized to SO_4^{2-} (Table 3), the reaction between Hg^{2+} and SO_4^{2-} was promoted to generate $HgSO_4$ which was a more stable mercury species in the solution. Moreover, $HgSO_4$ can be greatly hydrolyzed to form $Hg_3O_2SO_4$, a precipitate species of mercury, in the acidic solution [43]. With the absorption of SO_2 the pH value of the solution decreased to promote the Hg^0 oxidation which was in line with the results of pH value in Table 2. All these can explain the reason that the inhibited effect was weakened and the oxidation efficiency was improved at higher SO_2 concentration.

3.8.3. Effect of NO

The effect of NO concentration in simulated flue gas on Hg^0 oxidation was investigated experimentally and the results are shown in Fig. 4. As shown in the Figure that no significant variation of Hg^0 oxidation efficiency was observed with the increase of NO concentration from 0 to 800 ppm and the average Hg^0 oxidation efficiencies were maintained at about 93.0%.

When NO dissolved into the solution it would compete with Hg^0 for ·OH and H_2O_2 (Eqs. (32)–(36)) during the absorption process, leading to the decrease of ·OH for Hg^0 oxidation [23–25].

$$NO + {}^{\cdot}OH \rightarrow H^+ + NO_2^- \quad (32)$$

$$NO_2^- + {}^{\cdot}OH \rightarrow NO_3^- + {}^{\cdot}H \quad (33)$$

$$NO + {}^{\cdot}OH \rightarrow NO_2 + {}^{\cdot}H \quad (34)$$

$$NO_2^- + H_2O_2 \rightarrow NO_3^- + H_2O \quad (35)$$

$$NO_2 + {}^{\cdot}OH \rightarrow H^+ + NO_3^- \quad (36)$$

$$Hg^0 + 4HNO_3 \rightarrow Hg(NO_3)_2 + 2NO_2 + 2H_2O \quad (37)$$

Nevertheless, it has been postulated that the reaction of NO with Fenton's reagent can produce HNO_3, which can dissolve Hg^0 in the solution (Eq. (37)) [19,44]. In addition, some researchers have suggested that the Hg^0 absorption in aqueous oxidants catalyzed by Hg^{2+} was greatly enhanced with the presence of HNO_3 [45]. The favorable and unfavorable factors existed in the Fenton system might be counteracted with each other and exhibited a relatively stable Hg^0 oxidation efficiency.

Table 3
The analysis of ion products.

Ion products	SO_3^{2-}	SO_4^{2-}	NO_2^-	NO_3^-
IC concentration (mg/L)	0	683.50	0	113.57
Calculation concentration (mg/L)	–	771.43	–	121.27

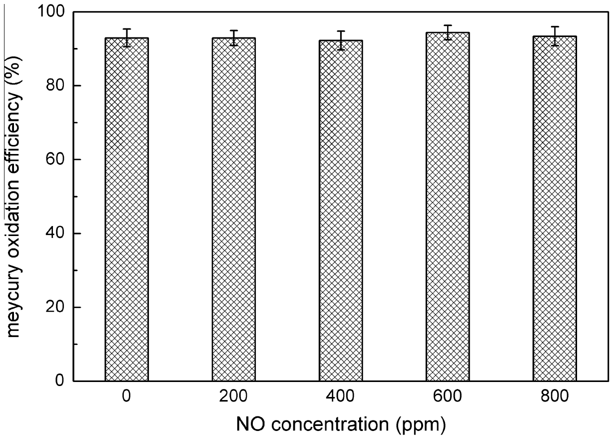

Fig. 4. Effect of the NO concentration on Hg^0 oxidation efficiency. Conditions: pH = 1; $[H_2O_2]$ = 0.05 mol/L; $[Fe^{2+}]/[H_2O_2]$ = 1/2; $[TiO_2]$ = 0.6 g/L; T = 40 °C; Q = 500 mL/min; 800 ppm SO_2; 9% O_2; C_{in} = 105 μg/m^3 and balance N_2.

3.9. Oxidation capacity and product analysis

The outlet concentrations of Hg^0, SO_2 and NO were tested by the mercury analyzer and a flue gas analyzer (Kane 950, UK), the analysis of ion products in the solution were carried out by using ion chromatography (IC) (Dionex ISC-900, USA) and spectrophotometry. The results are shown in Fig. 5 and Table 3.

As shown in Fig.5, the average removal efficiencies of Hg^0, SO_2 and NO were about 90%, 100% and 40% respectively. The results of product analysis showed that SO_2 and NO in the flue gas were removed by oxidation reaction and the main ion products in the solution were SO_4^{2-} and NO_3^-. The absence of SO_3^{2-} and NO_2^- in the solution may attribute to the instability of SO_3^{2-} and NO_2^- in H_2O_2 solution (Eqs. (26), (32) and (34)), which is consistent with the research results of Yangxian Liu [24,25].

In order to further verify the reaction pathways of SO_2 and NO in the Fenton system, based on the material balances of SO_2 and NO, the calculated concentrations of SO_4^{2-} and NO_3^- are shown in Table 3. It has been assumed that the removed SO_2 and NO com-

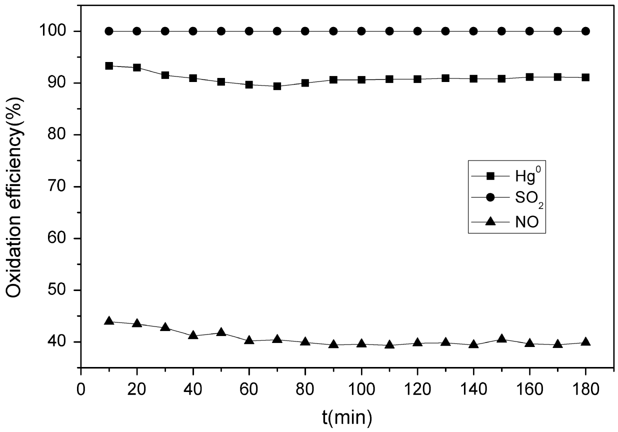

Fig. 5. The oxidation efficiencies of Hg^0, SO_2 and NO by UV/Fenton system. Conditions: pH = 1; $[H_2O_2]$ = 0.05 mol/L; $[Fe^{2+}]/[H_2O_2]$ = 1/2; $[TiO_2]$ = 0.6 g/L; T = 40 °C; Q = 500 mL/min; 1000 ppm SO_2; 600 ppm NO; 9% O_2; C_{in} = 105 μg/m^3 and balance N_2.

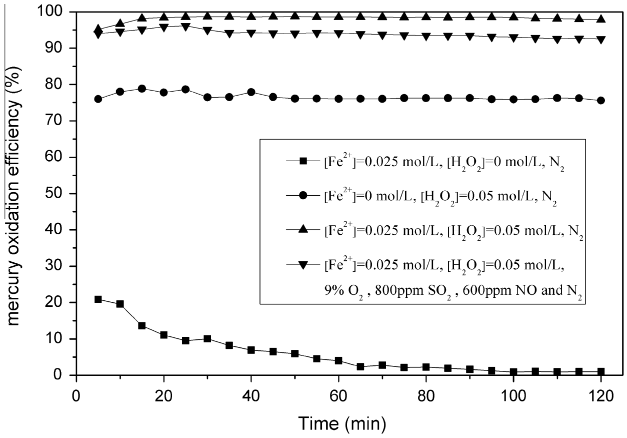

Fig. 6. Effects of different systems on Hg^0 oxidation efficiencies. Conditions: pH = 1; $[TiO_2]$ = 0.6 g/L; T = 40 °C; Q = 500 mL/min; C_{in} = 105 μg/m^3.

pletely converted to SO_4^{2-} and NO_3^- under the experimental condition. Compared with the actual values, the calculation concentrations are in good agreement with the results of IC.

4. Effect of different systems at optimal parameters

The Hg^0 oxidation efficiency as a function of time for UV/Fe^{2+}/H_2O, UV/H_2O_2 and UV/Fenton systems are shown in Fig. 6. It suggested that just a very small part of Hg^0 could be oxidized by UV/Fe^{2+}/H_2O system. For the UV/H_2O_2 system, about 76% of average oxidation efficiency was observed. The UV/Fenton system exhibited the highest oxidation efficiency in the absence of SO_2, NO and O_2 in the simulated flue gas. While with 800 ppm SO_2, 600 ppm NO and 9% O_2 in the flue gas the average Hg^0 oxidation efficiency decreased about 4.3% in the UV/Fenton system.

As a source of $^{\cdot}OH$ and $HO_2^{\cdot}$, H_2O_2 plays a very essential role in the Fenton system and little $^{\cdot}OH$ and $HO_2^{\cdot}$ could be generated in the absence of H_2O_2 resulting in low oxidation efficiency of Hg^0 in this system. Under the UV radiation the H_2O_2 could be promoted to decompose to $^{\cdot}OH$ and $HO_2^{\cdot}$ which then oxidized the Hg^0 in the solution. The Hg^0 oxidation efficiency had a sharp increase by adding 0.025 mol/L Fe^{2+} into the solution which was due to the catalytic effect of Fe^{2+} on the decomposition of H_2O_2 to generate $^{\cdot}OH$ and $HO_2^{\cdot}$.

5. Conclusions

The oxidation of Hg^0 by UV/Fenton system was studied in a lab-scale bubble reactor. The objective of the enhanced oxidation process was to convert the insoluble Hg^0 of coal-fired utility boiler flue gas into its soluble oxidized form and then to be co-effective removal with SO_2 by the WFGD. From the experimental results the following conclusions can be drawn:

(1) The Hg^0 oxidation efficiency decreased with the increase of initial solution pH value and flue gas rate, a suitable solution pH window was found between 1 and 3.
(2) Hg^0 oxidation process was firstly promoted by the increased of H_2O_2, TiO_2 and Fe^{2+} concentration to a certain value while decreased with the further increase of these parameters.
(3) The solution temperature had an essential influence on Hg^0 oxidation, and the lower Hg^0 oxidation efficiency at temperatures higher than 40 °C was due to the acceleration of H_2O_2 decomposition.
(4) The O_2 in the flue gas can promote the Hg^0 oxidation, but the oxidation efficiency was inhibited seriously when the O_2 concentration was higher than 9%.
(5) SO_2 has an inhibition effect on the mercury oxidation process, but the inhibition was weakened with the increase of the SO_2 concentration.
(6) NO has no obvious effect on Hg^0 oxidation under the experimental conditions.

Acknowledgments

This work was supported by the National High Technology Research and Development Program of China (863 Program) (No. 2011AA060803), Project 51278177 supported by the National Natural Science Foundation of China, The Scientific and Technological Major Special Project of Hunan Province in China (2010XK6003).

References

[1] E.G. Pacyna, J.M. Pacyna, K. Sundseth, J. Munthe, K. Kindbom, S. Wilson, F. Steenhuisen, P. Maxson, Global emission of mercury to the atmosphere from anthropogenic sources in 2005 and projections to 2020, Atmos. Environ. 44 (2010) 2487–2499.
[2] J.H. Pavlish, E.A. Sondreal, M.D. Mann, E.S. Olson, K.C. Galbreath, D.L. Laudal, S.A. Benson, State review of mercury control options for coal-fired power plants, Fuel Process. Technol. 82 (2003) 89–165.
[3] Z. Qu, N. Yan, P. Liu, J. Jia, S. Yang, The role of iodine monochloride for the oxidation of elemental mercury, J. Hazard. Mater. 183 (2010) 132–137.
[4] H.Q. Yang, Z.H. Xu, M.H. Fan, A.E. Bland, R.R. Judkins, Adsorbents for capturing mercury in coal-fired boiler flue gas, J. Hazard. Mater. 146 (2007) 1–11.
[5] US EPA. Final Mercury and Air Toxics Standards (MATS) for Power Plants. Final – Rule <http://www.epa.gov/airquality/powerplanttoxics/actions.html> (effective on 19.04.12).
[6] A.A. Presto, E.J. Granite, Survey of catalysts for oxidation of mercury in flue gas, Environ. Sci. Technol. 40 (2006) 5601–5609.
[7] R. Yan, D.T. Liang, L. Tsen, Y.P. Wong, Y.K. Lee, Bench-scale experimental evaluation of carbon performance on mercury vapour adsorption, Fuel 83 (2004) 2401–2409.
[8] H.C. Hsi, H.H. Lee, J.F. Hwang, W. Chen, Mercury speciation and distribution in a 660-megawatt utility boiler in Taiwan firing bituminous coals, J. Air Waste Manage. 60 (2010) 514–522.
[9] Y. Cao, B. Chen, J. Wu, H. Cui, J. Smith, C.K. Chen, P. Chu, W.P. Pan, Study of mercury oxidation by a selective catalytic reduction catalyst in a pilot-scale slipstream reactor at a utility boiler burning bituminous coal, Energy Fuel 21 (2007) 145–156.
[10] X. Xu, Q. Ye, T. Tang, D. Wang, Hg^0 oxidative absorption by $K_2S_2O_8$ solution catalyzed by Ag^+ and Cu^{2+}, J. Hazard Mater. 158 (2008) 410–416.
[11] R.R. Jensen, S. Karki, H. Salehfar, Artificial neural network-based estimation of mercury speciation in combustion flue gases, Fuel Process. Technol. 85 (2004) 451–462.
[12] H. Li, C.Y. Wu, Y. Li, J. Zhang, Superior activity of MnO_x–CeO_2/TiO_2 catalyst for catalytic oxidation of elemental mercury at low flue gas temperatures, Appl. Catal. B: Environ. 111–112 (2012) 381–388.
[13] L. Jia, R. Dureau, V. Ko, E.J. Anthony, Oxidation of mercury under ultraviolet (UV) irradiation, Energy Fuel 24 (2010) 4351–4356.
[14] H.C. Hsi, C.Y. Tsai, Synthesis of TiO_{2-x} visible-light photocatalyst using N_2/Ar/He thermal plasma for low-concentration elemental mercury removal, Chem. Eng. J 191 (2012) 378–385.
[15] Y.X. Zhao, M.D. Mann, E.S. Olson, J.H. Pavlish, G.E. Dunham, Effects of sulfur dioxide and nitric oxide on mercury oxidation and reduction under homogeneous conditions, J. Air Waste Manage. 56 (2006) 628–635.
[16] S.H. Liu, N.Q. Yan, Z.R. Liu, Z. Qu, P. Wang, S.G. Chang, C. Miller, Using bromine gas to enhance mercury removal from flue gas of coal-fired power plants, Environ. Sci. Technol. 41 (2007) 1405–1412.
[17] A.I. Martinez, B.K. Deshpande, Kinetic modeling of H_2O_2-enhanced oxidation of flue gas elemental mercury, Fuel Process Technol 88 (2007) 982–987.
[18] M. Vahedpour, M. Tozihi, F. Nazari, Mechanistic study on the ozone-mercury reaction and the effect of water and water dimer molecules, J. Chin. Chem. Soc.-Taip 58 (2011) 398–407.
[19] Nick D. Hutson, Renata Krzyzynska, A.R.K. Srivastava, Simultaneous removal of SO_2, NO_x, and Hg from coal flue gas using a $NaClO_2$-enhanced wet scrubber, Ind. Eng. Chem. Res 47 (2008) 5825–5831.
[20] P. Fang, C.P. Cen, Z.J. Tang, Experimental study on the oxidative absorption of Hg^0 by $KMnO_4$ solution, Chem. Eng. J. 198 (2012) 95–102.
[21] R.K. Srivastava, W. Jozewicz, C. Singer, SO_2 scrubbing technologies: a review, Environ. Prog. 20 (2001) 219–227.
[22] D. Lu, E.J. Anthony, Y. Tan, R. Dureau, V. Ko, M.A. Douglas, Mercury removal from coal combustion by Fenton reactions – Part A: Bench-scale tests, Fuel 86 (2007) 2789–2797.
[23] R.T. Guo, W.G. Pan, X.B. Zhang, J.X. Ren, Q. Jin, H.J. Xu, J. Wu, Removal of NO by using Fenton reagent solution in a lab-scale bubbling reactor, Fuel 90 (2011) 3295–3298.

[24] Y.X. Liu, J. Zhang, Photochemical oxidation removal of NO and SO_2 from simulated flue gas of coal-fired power plants by wet scrubbing using UV/H_2O_2 advanced oxidation process, Ind. Eng. Chem. Res. 50 (2011) 3836–3841.

[25] Y. Liu, J. Zhang, C. Sheng, Y. Zhang, L. Zhao, Simultaneous removal of NO and SO_2 from coal-fired flue gas by UV/H_2O_2 advanced oxidation process, Chem. Eng. J. 162 (2010) 1006–1011.

[26] Y. Samet, E. Hmani, R. Abdelhedi, Fenton and solar photo-Fenton processes for the removal of chlorpyrifos insecticide in wastewater, Water Sa 38 (2012) 537–542.

[27] X.W. Liu, X.F. Sun, D.B. Li, W.W. Li, Y.X. Huang, G.P. Sheng, H.Q. Yu, Anodic Fenton process assisted by a microbial fuel cell for enhanced degradation of organic pollutants, Water Res. 46 (2012) 4371–4378.

[28] Y.X. Liu, J. Zhang, Z.L. Wang, A study on kinetics of NO absorption from flue gas by using UV/Fenton wet scrubbing, Chem. Eng. J. 197 (2012) 468–474.

[29] Y.H. Zhong, X.L. Liang, Y. Zhong, J.X. Zhu, S.Y. Zhu, P. Yuan, H.P. He, J. Zhang, Heterogeneous UV/Fenton degradation of TBBPA catalyzed by titanomagnetite: catalyst characterization, performance and degradation products, Water Res. 46 (2012) 4633–4644.

[30] E. Neyens, J. Baeyens, A review of thermal sludge pre-treatment processes to improve dewaterability, J. Hazard. Mater. 98 (2003) 51–67.

[31] M.S. Lucas, J.A. Peres, Decolorization of the azo dye Reactive Black 5 by Fenton and photo-Fenton oxidation, Dyes Pigments 71 (2006) 236–244.

[32] E. Evgenidou, K. Fytianos, I. Poulios, Semiconductor-sensitized photodegradation of dichlorvos in water using TiO_2 and ZnO as catalysts, Appl. Catal. B-Environ. 59 (2005) 81–89.

[33] M.H. Habibi, H. Vosooghian, Photocatalytic degradation of some organic sulfides as environmental pollutants using titanium dioxide suspension, J. Photoch. Photobio. A 174 (2005) 45–52.

[34] M.I. Badawy, M.Y. Ghaly, T.A. Gad-Allah, Advanced oxidation processes for the removal of organophosphorus pesticides from wastewater, Desalination 194 (2006) 166–175.

[35] M. Muruganandham, M. Swaminathan, Decolourisation of reactive orange 4 by Fenton and photo-Fenton oxidation technology, Dyes Pigments 63 (2004) 315–321.

[36] Y. Zhao, C.M. Cao, Y.H. Han, Application of Fenton reaction technology in the field of environmental protection, in: Proceedings International Conference on Environmental Science and Information Application Technology, vol Iii, 2009, pp. 752–754.

[37] E. Evgenidou, E. Bizani, C. Christophoridis, K. Fytianos, Heterogeneous photocatalytic degradation of prometryn in aqueous solutions under UV–Vis irradiation, Chemosphere 68 (2007) 1877–1882.

[38] F.R. Carrillo-Pedroza, A.D. Sanchez, M. Soria-Aguilar, E.T.P. Trevino, Coal desulfurization in oxidative acid media using hydrogen peroxide and ozone: a kinetic and statistical approach, Energy Fuel 23 (2009) 3703–3710.

[39] M.S. Lucas, J.A. Peres, G. Li Puma, Treatment of winery wastewater by ozone-based advanced oxidation processes (O_3, O_3/UV and O_3/UV/H_2O_2) in a pilot-scale bubble column reactor and process economics, Sep. Purif. Technol. 72 (2010) 235–241.

[40] Y.G. Adewuyi, S.O. Owusu, Ultrasound-induced aqueous removal of nitric oxide from flue gases: effects of sulfur dioxide, chloride, and chemical oxidant, J. Phys. Chem. A 110 (2006) 11098–11107.

[41] S. Colle, J. Vanderschuren, D. Thomas, Simulation of SO_2 absorption into sulfuric acid solutions containing hydrogen peroxide in the fast and moderately fast kinetic regimes, Chem. Eng. Sci. 60 (2005) 6472–6479.

[42] J. Wo, M. Zhang, X. Cheng, X. Zhong, J. Xu, X. Xu, Hg^{2+} reduction and re-emission from simulated wet flue gas desulfurization liquors, J. Hazard. Mater. 172 (2009) 1106–1110.

[43] Y. Wang, Y. Liu, Z. Wu, J. Mo, B. Cheng, Experimental study on the absorption behaviors of gas phase bivalent mercury in Ca-based wet flue gas desulfurization slurry system, J. Hazard. Mater. 183 (2010) 902–907.

[44] C.D. Livengood, H.S. Huang, M.H. Mendelsohn, J.M. Wu, Enhancement of Mercury Control in Flue-Gas Cleanup Systems, Joint Power&Fuel Systems Contractors Conference, July 1996.

[45] L.L. Zhao, G.T. Rochelle, Mercury absorption in aqueous oxidants catalyzed by mercury(II), Ind. Eng. Chem. Res. 37 (1998) 380–387.